Photometric Analysis of Two Jupiter Sized Transiting Exoplanets and Creating "Current Model"

Hüseyin Avcu[1]

ABSTRACT

I report the photometric analysis of two exoplanets transiting the G-type stars K2-232 and Kepler-487. K2-232 star hosts a Jupiter-sized planet (K2-232 b), K2-232 planetary system is used to test the accuracy of "Current Model". Plots and parameters of both systems were obtained by using Current Model. Kepler-487 star hosts two different exoplanets, this paper focuses on Kepler-487 b (Jupiter-sized planet). These two exoplanets are especially interesting seeing that they orbit main-sequence stars in a close distance, these planets can be candidates for studies of evolution of gaseous planets and planetary migration.

Key Words: astronomical databases: miscellaneous – software: data analysis – techniques: photometric – stars: individual (K2-232) – stars: individual (Kepler 487)

[1]Private Temapark Bahçeşehir Science and Technology High School

1. INTRODUCTION

Understanding the planet that we live in and the Solar System of which it is a member has always been one of the most fundamental pursuits of science. Our desire to contribute to this effort is strengthened by the curiosity of finding other life forms other than ourselves. (Püsküllü 2016). For this reason, telescopes were developed and started to be used in the hope of finding other planets outside of our Solar System. These searches, which the telescopes continued with their non-stop monitoring of the sky, yielded results, and many planets outside of our Solar System were discovered and continuing to be discovered (Püsküllü 2016). In today's conditions, the search for planets outside of our Solar System is done with telescopes, which is the most important investigative tool of astronomy, and receivers attached to them and various other equipments (Püsküllü 2016). Exoplanets are small and very faint objects that usually orbit close to their stars. Although they reflect the light they receive from their stars, they are very difficult to view directly due to the very bright light of their stars. However, they can be relatively easier to detect indirectly by observing the star that they orbit. (Yu et al. 2018) Here are some methods used in exoplanet observations; radial velocity, transit photometry, pulsar timing, gravitational lensing, and direct imaging. (Table 1) In addition, by continuing the regular observations of exoplanets that are known to transit, the changes that can be seen at the time of transit may reveal the existence of other exoplanets and satellites in those systems. (Nesvorný 2009)

Table 1
Exoplanets found using different methods
(accessed July 8, 2021: https://exoplanets.nasa.gov/alien-worlds/ways-to-find-a-planet/)

Finding Methods	Planets Found
Transit	3343
Radial Velocity	866
Gravitational Microlensing	108
Direct Imaging	53
Astrometry	1

Observations made with the transit method is the most common method for discovering and analysing exoplanets. (Brown et al. 2001) As an exoplanet passes in front of the star it orbits, some of the light from the star is blocked, resulting in a slight decrease in flux. After the transition ends, the flux rises and then decreases again when the star is shrouded by the planet. (Winn 2010) (Fig. 1)

Figure 1 – Demonstration of the transit and occultation event (Winn 2010)

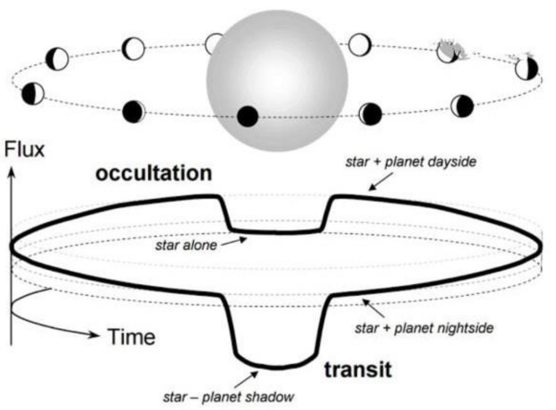

With the observations of transiting planets, a new field called transit photometry has emerged. With transit photometry, the start and end times of the exoplanet's transit in front of the star disk are calculated, and information about the geometry of the transition and the depth of the occultation are obtained. With this information, some planetary parameters of the transiting planetary systems are obtained by modelling the light curves. The transit light curve cannot provide information about the mass of the planet. (Fig. 2) (Winn 2010)

Figure 2 – Phase curve of the first extrasolar planet discovered to be transiting

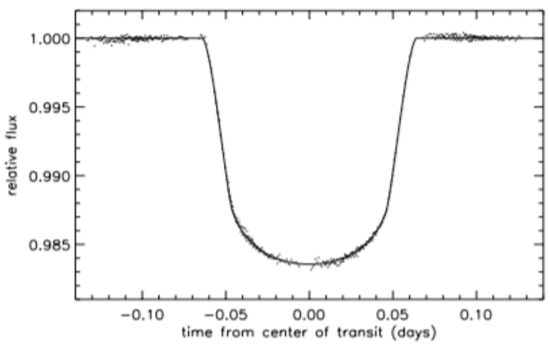

HD 209458 b (Brown et al. 2001)

For this reason, radial velocity observation is required in addition to the light curve. It is possible to tell the information about the atmosphere of the exoplanet and the surface temperature with spectral study. The radius of the planet is obtained from photometric observations, and the mass of the planet is obtained from observations of radial velocity. Thus, the density of the planet can be calculated and its internal structure can be modelled (Winn 2010).

After the first discovery of exoplanets, exoplanets and stars have been included in the literature with both special and general evaluations. Because of ground and space-based observational missions. while ~10 exoplanets were discovered in 1996, this number increased to ~100 in 2003; In 2014, it increased to ~1000. As of 2021, the number of known exoplanets is around 4400 (accessed July 8, 2021: http://exoplanetarchive.ipac.caltech.edu/) The basic parameters of planets are mass and radius. By determining these two parameters, information about the internal structure, formation and evolution of the planet can be obtained by knowing the other astrophysical criteria and stellar parameters of a star. For this reason, the most common classification used for exoplanets is made using mass and radius distributions. (Table 2)

In this classification, Solar System planets areused and planets are separated according to their types in mass and radius ranges (Fressin et al. 2013).

A newly discovered exoplanet is named after the star it orbits. The first exoplanet discovered to orbit a star is named by adding the letter 'b' next to the name of the star. The other exoplanet discovered later in the same system is named by adding the letter 'c' to the end. In multi-planet systems, planets are labeled with the letters 'b, c, d…' in order of concentration (Saral 2012). However, exoplanets discovered in and around a star may have different names and often include the names of the projects in which they were discovered. For example, one of the stars in The Two Micron All Sky Survey catalog, known as 2MASS 19021775+3824032, is also one of the stars observed by the Kepler Space Telescope and is also named KIC 3323887 or Kepler-9. For example, WASP-1 b is the first exoplanet discovered by the WASP project. Similarly, HAT-P-32 b is the 32nd planet discovered by the HAT-NET Project (Saral 2012). One of the main purposes of the Kepler Space Telescope is to determine the existence of Earth-like and larger planets in the belt that can host life around Sun-like stars, and to obtain

Table 2
Common classifications for exoplanets (Mendez 2011)

Type	Mass ($M_\oplus$)	Radius ($R_\oplus$)
Terran	0.5 – 2	0.8 – 1.9
Superterran	2 – 10	1.3 – 3.3
Jovian	10 – 50	2.1 – 5.7
Neptunian	50 – 5000	3.5 – 27

statistical information about the periods and radii of these planets. The Kepler Space Telescope has observed 1/400 of the entire sky. The region Kepler observes is the region where the Cygnus and the Lyga constellations are located. Here, as a result of the observation of 156000 previously determined stars between 12 May and 17 September 2009, 4424 planets has been discovered (as of July 8, 2021). Of these, 165 are classified as Terrestrial, 1357 as Super Earth, 1494 as Neptune and 1403 as Gas Giant. (http://exoplanetarchive.ipac.caltech.edu/)

1.1 *K2-232 b Exoplanet*

A team of astronomers led by Liang Yu from the Massachusetts Institute of Technology (MIT) detected transit signals in the light curves of K2-232, based on data from the space-based Kepler telescope (Yu et al. 2018). It was included in the Exoplanet Archive as K2-232 b, named after the host star. This newly found alien world is a hot, low-density Jovian (Jupiter-like) planet orbiting the bright star K2-232 (Yu et al. 2018). With its bright star, low planetary density, and large astronomical-scale height, the system is suitable for photometric examination. (Yu et al. 2018) (Fig. 3)

Figure 3 – Calibrated K2 photometry of HD 286123 (top), with vertical ticks indicating the locations of the transits, and phase-folded photometry and best-fitting light curve model (bottom) (Yu et al. 2018)

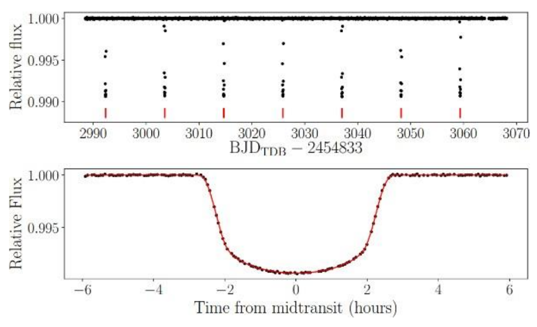

K2-232 b, is an exoplanet about the size of Jupiter orbiting the star K2-232, it was discovered in 2017 using the transit photometry method (Yu et al. 2018). K2-232 b is 434 light-years from Earth, It orbits 6.4 Gyr old, G0V* type star (Pecaut & Mamajek 2013; Yu et al. 2018) and it is on an elliptical orbit at a distance of 0.1 AU, it completes one orbit around the star in 11.2 days. It has a mass of 0.6 Jupiter masses, a radius of about 1.08 Jupiter radii, and an equilibrium temperature of 5.855 K. (Yu et al. 2018) (Table 3)

Table 3
Median values and 68% confidence intervals for parameters of K2-232 system (Yu et al. 2018)

Parameter	Units	HD 286123
Stellar Parameters		
M_*	Mass ($M_\odot$)	$1.062^{+0.047}_{-0.043}$
R_*	Radius ($R_\odot$)	$1.252^{+0.044}_{-0.043}$
ρ_*	Density (cgs)	$0.764^{+0.092}_{-0.082}$
$\log g$	Surface gravity (cgs)	4.270 ± 0.036
$T_{\rm eff}$	Effective Temperature (K)	5855^{+75}_{-86}
$[Fe/H]$	Metallicity	0.058 ± 0.058
L_*	Luminosity ($L_\odot$)	$1.66^{+0.13}_{-0.12}$
Age	Age (Gyr)	$6.5^{+1.8}_{-1.7}$
A_v	V-band extinction	$0.016^{+0.012}_{-0.011}$
σ_{SED}	Error scaling for SED photometry	$3.40^{+1.4}_{-0.85}$
d	Distance (pc)	$133.1^{+4.0}_{-3.9}$
π	Parallax (mas)	$7.52^{+0.23}_{-0.22}$
Planet Parameters		
a	Semi-major axis (AU)	0.0998 ± 0.0014
P	Period (days)	11.168453 ± 0.000018
M_P	Mass (M_J)	$0.408^{+0.049}_{-0.047}$
R_P	Radius (R_J)	$1.080^{+0.038}_{-0.037}$
e	Eccentricity	$0.268^{+0.036}_{-0.038}$
ω_*	Argument of Periastron (Degrees)	$168.6^{+6.4}_{-7.9}$
i	Inclination (Degrees)	$89.84^{+0.11}_{-0.16}$
ρ_P	Density (cgs)	$0.400^{+0.046}_{-0.043}$
$\log g_P$	Surface gravity (cgs)	$2.937^{+0.043}_{-0.045}$
T_{eq}	Equilibrium temperature (K)	999 ± 17
Θ	Safronov Number	$0.0708^{+0.0077}_{-0.0075}$
$\langle F \rangle$	Incident Flux (10^9 erg s^{-1} cm^{-2})	0.211 ± 0.013
T_C	Time of Transit (BJD$_{\rm TDB}$)	$2457858.856818 \pm 0.000037$
T_P	Time of Periastron (BJD$_{\rm TDB}$)	$2457860.45^{+0.26}_{-0.22}$
T_S	Time of eclipse (BJD$_{\rm TDB}$)	$2457862.59^{+0.26}_{-0.24}$
T_A	Time of Ascending Node (BJD$_{\rm TDB}$)	2457855.38 ± 0.17
T_D	Time of Descending Node (BJD$_{\rm TDB}$)	$2457860.62^{+0.17}_{-0.15}$
K	RV semi-amplitude (m/s)	$36.9^{+5.0}_{-4.6}$
$\log K$	Log of RV semi-amplitude	$1.568^{+0.055}_{-0.058}$
$e \cos \omega_*$		$-0.263^{+0.037}_{-0.034}$
$e \sin \omega_*$		$0.045^{+0.033}_{-0.034}$
$M_P \sin i$	Minimum mass (M_J)	$0.408^{+0.049}_{-0.047}$
M_P/M_*	Mass ratio	$0.000366^{+0.000047}_{-0.000044}$
R_P/R_*	Radius of planet in stellar radii	$0.08868^{+0.00011}_{-0.00010}$
a/R_*	Semi-major axis in stellar radii	$17.14^{+0.66}_{-0.64}$
d/R_*	Separation at mid transit	$15.2^{+1.3}_{-1.2}$
b	Impact parameter	$0.041^{+0.043}_{-0.029}$
δ	Transit depth (fraction)	0.007864 ± 0.000019
T_{FWHM}	FWHM duration (days)	$0.19100^{+0.00023}_{-0.00022}$
τ	Ingress/egress duration (days)	$0.016985^{+0.00010}_{-0.000030}$
T_{14}	Total duration (days)	$0.20802^{+0.00024}_{-0.00023}$
b_S	Eclipse impact Parameter	$0.045^{+0.047}_{-0.031}$
$T_{S,FWHM}$	Eclipse FWHM duration (days)	0.209 ± 0.014
τ_S	Eclipse ingress/egress duration (days)	$0.0186^{+0.0013}_{-0.0012}$
$T_{S,14}$	Total eclipse duration (days)	$0.228^{+0.016}_{-0.015}$
$\delta_{S,3.6\mu m}$	Blackbody eclipse depth at 3.6μm (ppm	$138.5^{+9.4}_{-9.1}$
$\delta_{S,4.5\mu m}$	Blackbody eclipse depth at 4.5μm (ppm	242 ± 13
Wavelength Parameters	Kepler	
$u_{1,Kepler}$	Linear limb-darkening coeff	0.433 ± 0.012
$u_{2,Kepler}$	Quadratic limb-darkening coeff	0.100 ± 0.027
Telescope Parameters	Kepler	
γ	APF instrumental offset (m/s)	-12.4 ± 2.2
γ	HIRES instrumental offset (m/s)	—
σ_J	APF RV jitter	$3.5^{+1.5}_{-1.4}$
σ_J	HIRES RV jitter	—
σ_J^2	APF RV jitter variance	$12.1^{+13}_{-7.7}$
σ_J^2	HIRES RV jitter variance	—
Transit Parameters	Kepler	
σ^2	Added variance	$0.00000000052^{+0.00000000016}_{-0.00000000014}$
F_0	Baseline flux	1.0000006 ± 0.0000028

1.2 *Kepler-487 b Exoplanet*

Kepler-487 b was discovered in 2016 by the Kepler space telescope using the transit method. It is the first of two planets orbiting a G-type star called Kepler-487 (Timothy et al. 2016) While manydetails are not yet known about this system, the probability of a false positive is very low. (Timothy et al. 2016) (Table 4)

Table 4
Some parameters of Kepler-487 b (accessed January 28, 2021: https://exoplanets.nasa.gov/exoplanet-catalog/5609/kepler-487-b/)

Planet Classification	Gas Giant
Discovery Date	2016
Mass	Unknown
Radius	1.019 M_J
Orbital Radius	Unknown
Orbital Period	15.4 Days

2. PURPOSE OF THE RESEARCH

The primary aim of this research is to analyse the light curve of Kepler 487 and present our contribution to literature by using it to establish the parameters of Kepler-487 b. After analysing the light curve, "Current Model" is used to obtain parameters of Kepler-487 b.
In line with this purpose, the primary goal of the research is; analysing K2-232 planetary system with "Current Model" and proving that "Current Model" has enough accuracy by comparing the results with other studies.
Thus; This new model, which has been proven to be accurate on the K2-232 system, has provided the basic parameters of the Kepler 487-b exoplanet.

2.1 *Research Question*

Can the fundamental parameters of Kepler-487 b exoplanet be determined by the transit photometry method applied for the analysis of K2-232 b exoplanet, which has been observed with the Kepler space telescope but not yet studied extensively? A current model was created to test the research question and validate the hypothesis. Because of the "Current Model" created, the basic parameters of the K2-232 b exoplanet were obtained using the photometric method and the model was verified by comparing the results with the values in the literature. The "Current Model", the accuracy of which was tested on K2-232 b exoplanet, was used for Kepler-487 b exoplanet and its contribution to the literature was presented by obtaining the basic parameters of the system.

2.2 *Hypothesis*

The "Current Model" that was proven in accuracy by comparing the results from K2-232 planetary system, is used to obtain basic parameters of Kepler-487 b.

3. METHOD

In this research, light curves will be analysed and the basic parameters of planetary systems will be evaluated, because of the "Current Model" created using Python (on Jupyter Notebook). (Table 5)

Table 5
Diagram of "Current Model"

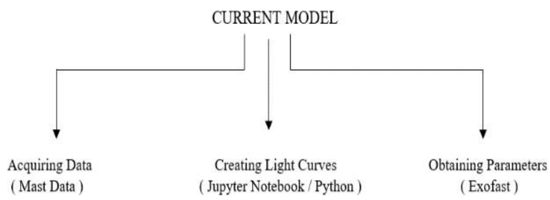

Current Model; It was carried out by the student who made and reported the project on modern, quad core, 7th generation 2.60 GHz processor and 16 GB RAM. Processes were repeated for each system.

3.1 *Obtaining Data*

Mast Data was used to access the optical data of Kepler-487 and K2-232 stars, which are used within the scope of the project and are known to have transiting planets. (https://archive.stsci.edu/) (Fig. 4)

3.2 *Creating a Light Curve*

In order to examine the target pixel file uploaded to the computer using MAST, Python code was made to turn tpf file into a light curve.

Figure 4 – Single frame from a target pixel file

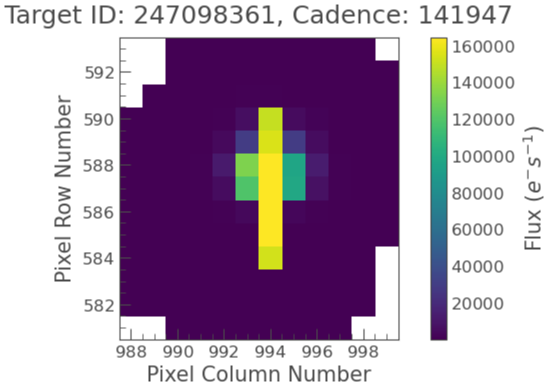

3.3 *Obtaining Parameters*

EXOFAST program was used to obtain the parameters of planetary systems (https://exoplanetarchive.ipac.caltech.edu/)
In this project, a "Current Model" was created for the parameters and analysis of selected planetary systems. To create the "Current Model"; Data was obtained using MAST (Mikulski Archive for Space Telescopes).
Code to process the light curve data was written in the Jupyter Notebook program using the Python language. EXOFAST was used to analyse the calibrted light curves. Each of the processes was repeated for selected planetary systems. (Eastman, Gaudi & Algol 2013; Kluvyer et al. 2016; Van Rossum & Drake 2009)

4. FINDINGS

This research consists of two stages: First step is proving the accuracy of "Current Model" by comparing parameters of K2-232 system that has been obtained using "Current Model" with values in the literature. Second step is to apply "Current Model" on Kepler 487 to obtain and analyse parameters of the system.

4.1 *Creating and Calibrating Light Curve of K2-232 System*

Python code has been written on Jupyter notebook for creating and calibrating light curve of K2-232 system. (Fig. 5)
Then a periodogram was created to see the orbital period of K2-232 b exoplanet. (Fig. 6)

Figure 5 – Calibrated light curve of K2-232

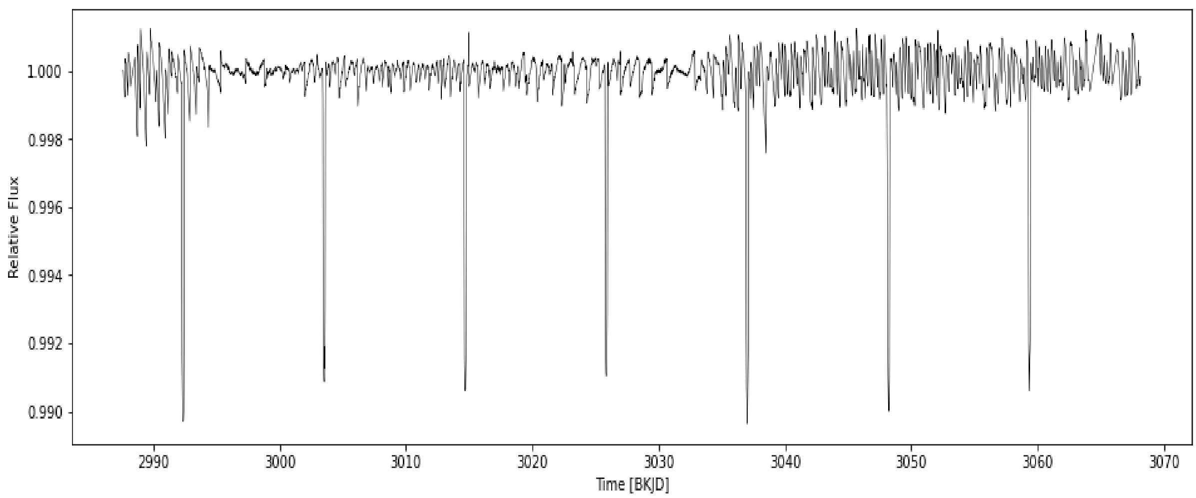

Figure 6 – Periodogram of Fig. 5 (Blue line indicates largest peak, red line indicates other considerable peaks)

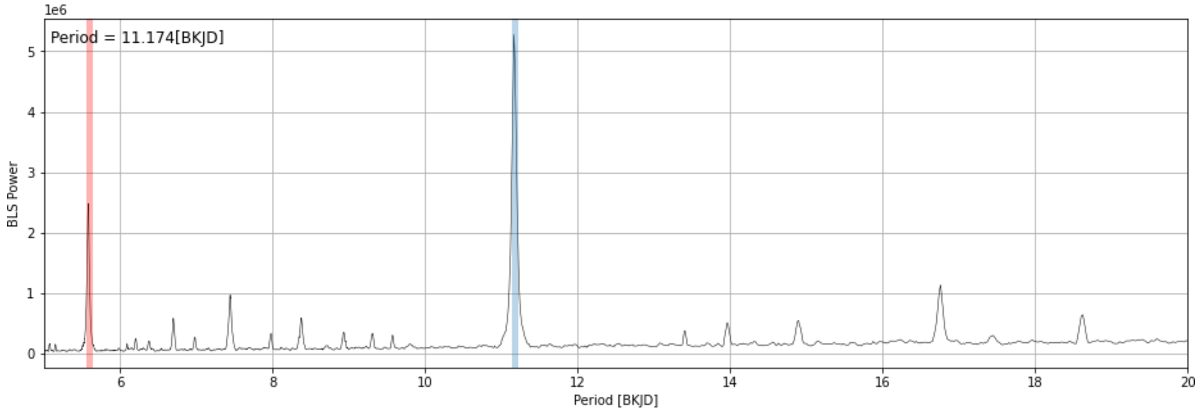

4.2 *Obtaining Paramters From The Light Curve*

First, calibrated light curve that has been obtained from the previous process is exported as ".fits" file. The file was then loaded to EXOFAST (Eastman et al. 2013) to obtain the parameters of K2-232 system. Input parameters for the host star were obtained from ExoFOP (Huber et al. 2016). See Fig. 7 for the transit and Table 6 formedian values for the parameter of K2-232 system.

Table 6
Median values and 68% confidence interval for K2-232 System

MEDIAN VALUES AND 68% CONFIDENCE INTERVAL FOR EXOFAST.

Parameter	Units	Value
Stellar Parameters:		
M_*	Mass ($M_\odot$)	$1.188^{+0.057}_{-0.055}$
R_*	Radius ($R_\odot$)	$1.167^{+0.042}_{-0.039}$
L_*	Luminosity ($L_\odot$)	$1.76^{+0.16}_{-0.15}$
ρ_*	Density (cgs)	$1.054^{+0.082}_{-0.075}$
$\log(g_*)$	Surface gravity (cgs)	4.378 ± 0.020
$T_{\rm eff}$	Effective temperature (K)	6153 ± 60
[Fe/H]	Metalicity	0.101 ± 0.039
Planetary Parameters:		
e	Eccentricity	$0.555^{+0.16}_{-0.085}$
ω_*	Argument of periastron (degrees)	-100^{+38}_{-25}
P	Period (days)	11.16882 ± 0.00037
a	Semi-major axis (AU)	0.1035 ± 0.0016
R_P	Radius (R_J)	$1.109^{+0.044}_{-0.040}$
T_{eq}	Equilibrium Temperature (K)	996^{+17}_{-16}
$\langle F \rangle$	Incident flux (10^9 erg s^{-1} cm^{-2})	$0.165^{+0.021}_{-0.025}$
RV Parameters:		
$e\cos\omega_*$		$-0.08^{+0.35}_{-0.30}$
$e\sin\omega_*$		$-0.505^{+0.055}_{-0.074}$
T_P	Time of periastron ($\rm BJD_{TDB}$)	$2457828.1^{+2.7}_{-5.6}$
Primary Transit Parameters:		
T_C	Time of transit ($\rm BJD_{TDB}$)	$2457825.3504^{+0.0028}_{-0.0032}$
R_P/R_*	Radius of planet in stellar radii	$0.0978^{+0.0012}_{-0.0014}$
a/R_*	Semi-major axis in stellar radii	$19.08^{+0.48}_{-0.47}$
u_1	linear limb-darkening coeff	$0.347^{+0.050}_{-0.049}$
u_2	quadratic limb-darkening coeff	0.301 ± 0.049
i	Inclination (degrees)	$88.29^{+0.12}_{-0.31}$
b	Impact Parameter	$0.782^{+0.022}_{-0.030}$
δ	Transit depth	$0.00957^{+0.00023}_{-0.00027}$
T_{FWHM}	FWHM duration (days)	$0.1880^{+0.0037}_{-0.0036}$
τ	Ingress/egress duration (days)	$0.0495^{+0.0053}_{-0.0057}$
T_{14}	Total duration (days)	$0.2376^{+0.0037}_{-0.0039}$
P_T	A priori non-grazing transit prob	$0.0348^{+0.0061}_{-0.0026}$
$P_{T,G}$	A priori transit prob	$0.0423^{+0.0075}_{-0.0031}$
F_0	Baseline flux	0.999989 ± 0.000010
Secondary Eclipse Parameters:		
T_S	Time of eclipse ($\rm BJD_{TDB}$)	$2457828.5^{+2.5}_{-5.9}$
b_S	Impact parameter	$0.259^{+0.032}_{-0.049}$
$T_{S,FWHM}$	FWHM duration (days)	$0.099^{+0.010}_{-0.018}$
τ_S	Ingress/egress duration (days)	$0.0104^{+0.0012}_{-0.0021}$
$T_{S,14}$	Total duration (days)	$0.109^{+0.012}_{-0.020}$
P_S	A priori non-grazing eclipse prob	$0.102^{+0.049}_{-0.014}$
$P_{S,G}$	A priori eclipse prob	$0.125^{+0.059}_{-0.017}$

Figure 7 – Calibrated light curve and best-fitting model (shown on red) (top), residuals (bottom)

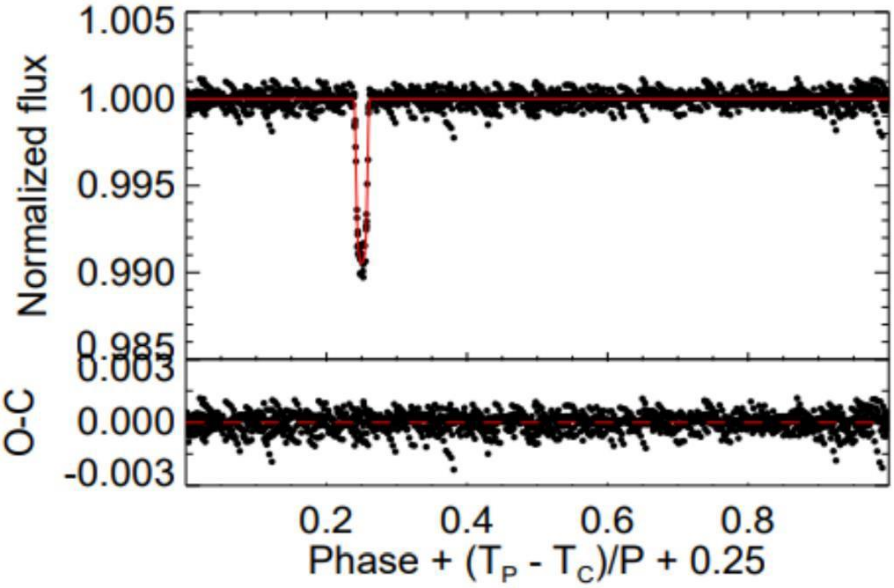

4.3 *Comparing The Results*

Parameters of K2-232 that is obtained from EXOFAST is then compared with the parameters of other studies (Yu et al. 2018) to prove the accuracy of "Current Model" see Table 7 and 8 for comparison between two results.

Table 7 Parameters that has been obtained by us

Parameter	Units	Value
Stellar Parameters:		
M_*	Mass ($M_\odot$)	$1.188^{+0.057}_{-0.055}$
R_*	Radius ($R_\odot$)	$1.167^{+0.042}_{-0.039}$
L_*	Luminosity ($L_\odot$)	$1.76^{+0.16}_{-0.15}$
ρ_*	Density (cgs)	$1.054^{+0.082}_{-0.075}$
$\log(g_*)$	Surface gravity (cgs)	4.378 ± 0.020
T_{eff}	Effective temperature (K)	6153 ± 60
[Fe/H]	Metalicity	0.101 ± 0.039
Planetary Parameters:		
e	Eccentricity	$0.555^{+0.16}_{-0.085}$
ω_*	Argument of periastron (degrees)	-100^{+38}_{-25}
P	Period (days)	11.16882 ± 0.00037
a	Semi-major axis (AU)	0.1035 ± 0.0016
R_P	Radius (R_J)	$1.109^{+0.044}_{-0.040}$
T_{eq}	Equilibrium Temperature (K)	996^{+17}_{-16}
$\langle F \rangle$	Incident flux (10^9 erg s^{-1} cm^{-2})	$0.165^{+0.021}_{-0.025}$
RV Parameters:		
$e\cos\omega_*$		$-0.08^{+0.35}_{-0.30}$
$e\sin\omega_*$		$-0.505^{+0.055}_{-0.074}$
T_P	Time of periastron ($\mathrm{BJD_{TDB}}$)	$2457828.1^{+2.7}_{-5.6}$
Primary Transit Parameters:		
T_C	Time of transit ($\mathrm{BJD_{TDB}}$)	$2457825.3504^{+0.0028}_{-0.0032}$
R_P/R_*	Radius of planet in stellar radii	$0.0978^{+0.0012}_{-0.0014}$
a/R_*	Semi-major axis in stellar radii	$19.08^{+0.48}_{-0.47}$
u_1	linear limb-darkening coeff	$0.347^{+0.050}_{-0.049}$
u_2	quadratic limb-darkening coeff	0.301 ± 0.049
i	Inclination (degrees)	$88.29^{+0.12}_{-0.31}$
b	Impact Parameter	$0.782^{+0.022}_{-0.030}$
δ	Transit depth	$0.00957^{+0.00023}_{-0.00027}$
T_{FWHM}	FWHM duration (days)	$0.1880^{+0.0037}_{-0.0036}$
τ	Ingress/egress duration (days)	$0.0495^{+0.0053}_{-0.0057}$
T_{14}	Total duration (days)	$0.2376^{+0.0037}_{-0.0039}$
P_T	A priori non-grazing transit prob	$0.0348^{+0.0061}_{-0.0026}$
$P_{T,G}$	A priori transit prob	$0.0423^{+0.0075}_{-0.0031}$
F_0	Baseline flux	0.999989 ± 0.000010
Secondary Eclipse Parameters:		
T_S	Time of eclipse ($\mathrm{BJD_{TDB}}$)	$2457828.5^{+2.5}_{-5.9}$
b_S	Impact parameter	$0.259^{+0.032}_{-0.049}$
$T_{S,FWHM}$	FWHM duration (days)	$0.099^{+0.010}_{-0.018}$
τ_S	Ingress/egress duration (days)	$0.0104^{+0.0012}_{-0.0021}$
$T_{S,14}$	Total duration (days)	$0.109^{+0.012}_{-0.020}$
P_S	A priori non-grazing eclipse prob	$0.102^{+0.049}_{-0.014}$
$P_{S,G}$	A priori eclipse prob	$0.125^{+0.059}_{-0.017}$

Table 8 Parameters that was obtained by (Yu et al. 2018)

Parameter	Units	HD 286123
Stellar Parameters		
M_*	Mass ($M_\odot$)	$1.062^{+0.047}_{-0.043}$
R_*	Radius ($R_\odot$)	$1.252^{+0.044}_{-0.043}$
ρ_*	Density (cgs)	$0.764^{+0.092}_{-0.082}$
$\log g$	Surface gravity (cgs)	4.270 ± 0.036
T_{eff}	Effective Temperature (K)	5855^{+75}_{-86}
$[Fe/H]$	Metallicity	0.058 ± 0.058
L_*	Luminosity ($L_\odot$)	$1.66^{+0.13}_{-0.12}$
Age	Age (Gyr)	$6.5^{+1.8}_{-1.7}$
A_v	V-band extinction	$0.016^{+0.012}_{-0.011}$
σ_{SED}	Error scaling for SED photometry	$3.40^{+1.4}_{-0.85}$
d	Distance (pc)	$133.1^{+4.0}_{-3.9}$
π	Parallax (mas)	$7.52^{+0.23}_{-0.22}$
Planet Parameters		
a	Semi-major axis (AU)	0.0998 ± 0.0014
P	Period (days)	11.168453 ± 0.000018
M_P	Mass (M_J)	$0.408^{+0.049}_{-0.047}$
R_P	Radius (R_J)	$1.080^{+0.038}_{-0.037}$
e	Eccentricity	$0.268^{+0.036}_{-0.038}$
ω_*	Argument of Periastron (Degrees)	$168.6^{+6.4}_{-7.9}$
i	Inclination (Degrees)	$89.84^{+0.11}_{-0.16}$
ρ_P	Density (cgs)	$0.400^{+0.046}_{-0.043}$
$\log g_P$	Surface gravity (cgs)	$2.937^{+0.043}_{-0.045}$
T_{eq}	Equilibrium temperature (K)	999 ± 17
Θ	Safronov Number	$0.0708^{+0.0077}_{-0.0075}$
$\langle F \rangle$	Incident Flux (10^9 erg s^{-1} cm^{-2})	0.211 ± 0.013
T_C	Time of Transit ($\mathrm{BJD_{TDB}}$)	$2457858.856818 \pm 0.000037$
T_P	Time of Periastron ($\mathrm{BJD_{TDB}}$)	$2457860.45^{+0.26}_{-0.22}$
T_S	Time of eclipse ($\mathrm{BJD_{TDB}}$)	$2457862.59^{+0.26}_{-0.24}$
T_A	Time of Ascending Node ($\mathrm{BJD_{TDB}}$)	2457855.38 ± 0.17
T_D	Time of Descending Node ($\mathrm{BJD_{TDB}}$)	$2457860.62^{+0.17}_{-0.15}$
K	RV semi-amplitude (m/s)	$36.9^{+5.0}_{-4.6}$
$\log K$	Log of RV semi-amplitude	$1.568^{+0.055}_{-0.058}$
$e\cos\omega_*$		$-0.263^{+0.037}_{-0.034}$
$e\sin\omega_*$		$0.045^{+0.033}_{-0.034}$
$M_P \sin i$	Minimum mass (M_J)	$0.408^{+0.049}_{-0.047}$
M_P/M_*	Mass ratio	$0.000366^{+0.000047}_{-0.000044}$
R_P/R_*	Radius of planet in stellar radii	$0.08868^{+0.00011}_{-0.00010}$
a/R_*	Semi-major axis in stellar radii	$17.14^{+0.66}_{-0.64}$
d/R_*	Separation at mid transit	$15.2^{+1.3}_{-1.2}$
b	Impact parameter	$0.041^{+0.043}_{-0.029}$
δ	Transit depth (fraction)	0.007864 ± 0.000019
T_{FWHM}	FWHM duration (days)	$0.19100^{+0.00023}_{-0.00022}$
τ	Ingress/egress duration (days)	$0.016985^{+0.00010}_{-0.000030}$
T_{14}	Total duration (days)	$0.20802^{+0.00024}_{-0.00023}$
b_S	Eclipse impact Parameter	$0.045^{+0.047}_{-0.031}$
$T_{S,FWHM}$	Eclipse FWHM duration (days)	0.209 ± 0.014
τ_S	Eclipse ingress/egress duration (days)	$0.0186^{+0.0013}_{-0.0012}$
$T_{S,14}$	Total eclipse duration (days)	$0.228^{+0.016}_{-0.015}$
$\delta_{S,3.6\mu m}$	Blackbody eclipse depth at 3.6μm (ppm	$138.5^{+9.4}_{-9.1}$
$\delta_{S,4.5\mu m}$	Blackbody eclipse depth at 4.5μm (ppm	242 ± 13
Wavelength Parameters	Kepler	
$u_{1,Kepler}$	Linear limb-darkening coeff	0.433 ± 0.012
$u_{2,Kepler}$	Quadratic limb-darkening coeff	0.100 ± 0.027
Telescope Parameters	Kepler	
γ	APF instrumental offset (m/s)	-12.4 ± 2.2
γ	HIRES instrumental offset (m/s)	—
σ_J	APF RV jitter	$3.5^{+1.5}_{-1.4}$
σ_J	HIRES RV jitter	—
σ_J^2	APF RV jitter variance	$12.1^{+13}_{-7.7}$
σ_J^2	HIRES RV jitter variance	—
Transit Parameters	Kepler	
σ^2	Added variance	$0.00000000052^{+0.0000000016}_{-0.00000000014}$
F_0	Baseline flux	1.0000006 ± 0.0000028

4.4 *Applying The Same Method For Kepler-487 System*

Since "Current Model" was proven to be accurate on previous steps, we will now use it to obtain parameters of Kepler-487 system. See Fig. 8 for calibrated light curve, Fig. 9 for periodogram, Fig. 10 for transit fit and Table 9 for parameters of the Kepler-487 system that has been obtained using EXOFAST (Eastman et al. 2013). ExoFOP was used again to obtain the stellar parameters of the system. (accessed February 10, 2021: https://exofop.ipac.caltech.edu/tess/)

Figure 8 – Calibrated light curve of Kepler-487 system

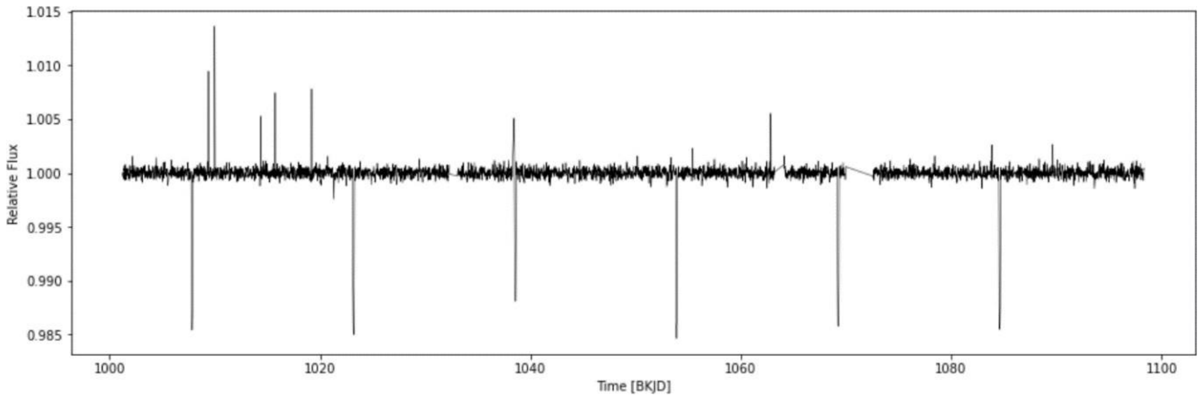

Figure 9 – Periodogram of Fig. 8 (Blue line indicates largest peak, red lines indicate other considerable peaks)

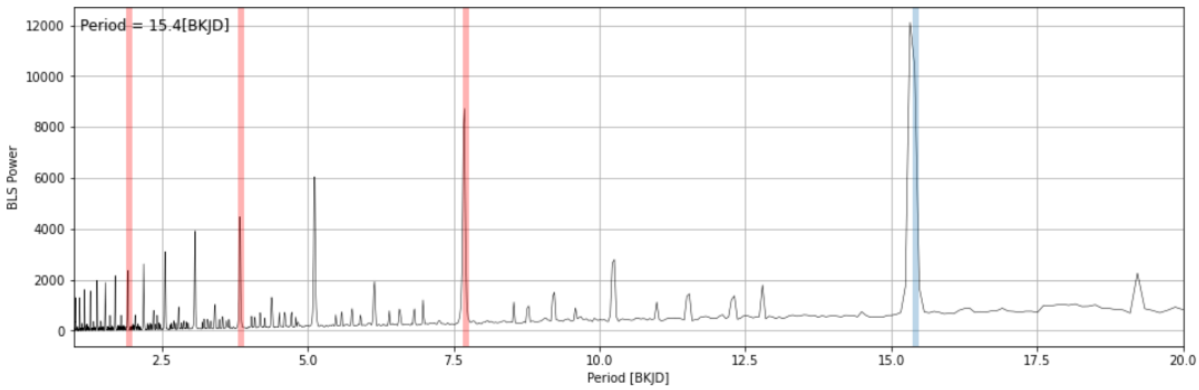

Figure 10 – Calibrated light curve and best-fitting model (shown on red) (top), residuals(bottom)

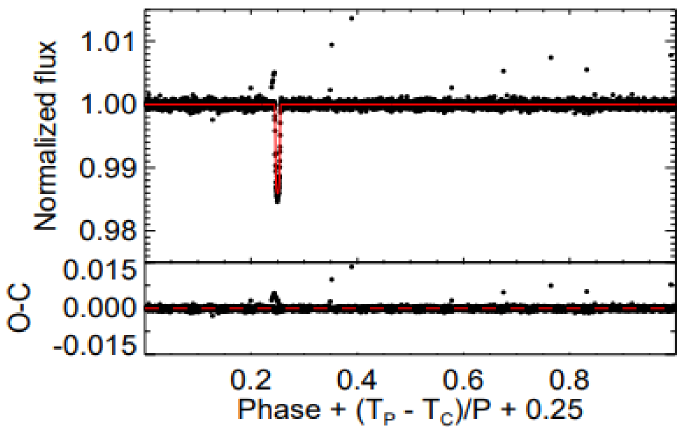

Table 9
Median values and 68% confidence interval for Kepler-487 system

MEDIAN VALUES AND 68% CONFIDENCE INTERVAL FOR EXOFAST.

Parameter	Units	Value
Stellar Parameters:		
M_*	Mass ($M_\odot$)	$0.940^{+0.053}_{-0.051}$
R_*	Radius ($R_\odot$)	$0.889^{+0.057}_{-0.055}$
L_*	Luminosity ($L_\odot$)	$0.621^{+0.096}_{-0.089}$
ρ_*	Density (cgs)	$1.89^{+0.35}_{-0.30}$
$\log(g_*)$	Surface gravity (cgs)	$4.514^{+0.050}_{-0.049}$
$T_{\rm eff}$	Effective temperature (K)	5433^{+84}_{-80}
[Fe/H]	Metalicity	0.00 ± 0.10
Planetary Parameters:		
e	Eccentricity	$0.23^{+0.36}_{-0.15}$
ω_*	Argument of periastron (degrees)	0^{+110}_{-170}
P	Period (days)	$15.35888^{+0.00030}_{-0.00024}$
a	Semi-major axis (AU)	0.1184 ± 0.0022
R_P	Radius (R_J)	$0.940^{+0.069}_{-0.065}$
T_{eq}	Equilibrium Temperature (K)	718^{+24}_{-23}
$\langle F \rangle$	Incident flux (10^9 erg s^{-1} cm^{-2})	$0.0547^{+0.0094}_{-0.011}$
RV Parameters:		
$e\cos\omega_*$		$0.00^{+0.38}_{-0.32}$
$e\sin\omega_*$		$0.024^{+0.097}_{-0.17}$
T_P	Time of periastron ($\rm BJD_{TDB}$)	$2453580.3^{+5.6}_{-4.7}$
Primary Transit Parameters:		
T_C	Time of transit ($\rm BJD_{TDB}$)	2453590^{+47}_{-39}
R_P/R_*	Radius of planet in stellar radii	$0.1079^{+0.0030}_{-0.0016}$
a/R_*	Semi-major axis in stellar radii	$28.7^{+1.7}_{-1.6}$
u_1	linear limb-darkening coeff	$0.466^{+0.047}_{-0.045}$
u_2	quadratic limb-darkening coeff	$0.226^{+0.054}_{-0.050}$
i	Inclination (degrees)	$89.30^{+0.44}_{-0.41}$
b	Impact Parameter	0.30 ± 0.20
δ	Transit depth	$0.01164^{+0.00066}_{-0.00035}$
T_{FWHM}	FWHM duration (days)	$0.1472^{+0.0016}_{-0.0018}$
τ	Ingress/egress duration (days)	$0.0175^{+0.0044}_{-0.0016}$
T_{14}	Total duration (days)	$0.1653^{+0.0033}_{-0.0022}$
P_T	A priori non-grazing transit prob	$0.0356^{+0.0091}_{-0.0054}$
$P_{T,G}$	A priori transit prob	$0.0442^{+0.011}_{-0.0066}$
F_0	Baseline flux	1.000020 ± 0.000010
Secondary Eclipse Parameters:		
T_S	Time of eclipse ($\rm BJD_{TDB}$)	2453577.0 ± 5.1
b_S	Impact parameter	$0.29^{+0.18}_{-0.19}$
$T_{S,FWHM}$	FWHM duration (days)	$0.153^{+0.032}_{-0.039}$
τ_S	Ingress/egress duration (days)	$0.0194^{+0.0038}_{-0.0061}$
$T_{S,14}$	Total duration (days)	$0.173^{+0.033}_{-0.046}$
P_S	A priori non-grazing eclipse prob	$0.0314^{+0.025}_{-0.0031}$
$P_{S,G}$	A priori eclipse prob	$0.0392^{+0.033}_{-0.0040}$

5. DISCUSSION and CONCLUSION

In this research, light curves were analysed with "Current Model" that was created using python, python packages (Cardoso et al. 2018; Harris et al. 2021; Hunter et al. 2007; Price-Whelan et al. 2018; Robitaille et al. 2013; Winn 2010; Foreman-Mackey et al. 2021) and EXOFAST (Eastman et al. 2013). The "Current Model", which has been proven to be accurate for the K2-232 b exoplanet, has completed the literature gaps for Kepler 487 b exoplanet. Theoptical data of K2-232 was acquired using MAST, and a light curve was created with the code written in the Jupyter Notebook program using the Python language (Kluvyer et al. 2016; Van Rossum & Drake 2009). In order to calculate the parameters of exoplanet K2-232 b more precisely, it is necessary to prevent noise and other factors that harms the data, it is also important to not over-process the data because over-processing may effect the end result badly. For this reason raw light curve was calibrated carefully. (Fig 5)
The periodogram was obtained with the written code and as a result of the analysis, it was determined that orbital period of the K2-232 b exoplanet was 11,254 days. (Fig 6)
Some of the parameters obtained differ slightly from the values in literature. However, it was mostly found within/near the error limits.
Considering that the analysis methods used on other studies with different light curves and different initial planetary system parameters, it is observed that the parameters are largely compatible. The optical data of Kepler 487 star was acquired using MAST, and the target pixel file was turned into a light curve using the code that was written with Python language in the Jupyter Notebook program. In order to calculate the parameters of exoplanet Kepler- 487 b more precisely, it is necessary to prevent noise and other factors that harms the data. Forthis reason raw light curve was calibrated. (Fig. 8)
The periodogram was obtained with the written code and as a result of the analysis, it was determined that the orbital period of Kepler 487 b exoplanet was 15,358 days. (Fig. 9)
The basic parameters of Kepler 487 b exoplanet and Kepler 487 star obtained with the "Current Model" have been established. (Table 9) In this research, the parameters of the host stars were also calculated in order to determinethe orbital and planetary parameters. (Table 9). Since the “Current Model” created within the scope of the project is focused on light curves. Mass, surface temperature and atmospheric properties of the exoplanet could not be analysed. For this, in addition to the light curve, radial velocity and spectral analysis are required. However, it has been proven that the "Current Model" can be used as an alternative in the analysis of transiting exoplanets. In addition these two planets can be good candidates for analysing planetary migration and evolution of gaseous planets because of their bright host stars, close orbit and their size (Yu et al. 2018).It is also necessary to maximize scientific accesibility and productivity of astronomical data, this would allow everyone to access and analyse astronomical data easily therefore new discoveries can be made easier and would allow everyone to learn more about astronomy.

ACKNOWLEDGEMENTS

In the making of this project; I would like to thank my advisor, Neslihan Yıldırım, The Physics teacher of Istanbul Private Temapark Bahçeşehir Science and Technology High School, Ekinsu Kaplan The Physics teacher of Istanbul Private Temapark. Bahçeşehir Science and Technology High School for helping in translation and Cem Özkurt, Head of the Physics Department of Istanbul Private Temapark Bahçeşehir Science and Technology High School. I also would like to express my deep gratitude to Professor Eda Sonbaş, Adıyaman University, Department of Physics for not sparing her suggestions and support during my research. This research made use of Lightkurve, a Python package for Kepler and TESS data analysis (Cardoso et al. 2018) This research made use of astropy (https://www.astropy.org) a community-developed core Python package for Astronomy. This research made use of NASA Exoplanet Archive and the Exoplanet Follow-up Observing Program (ExoFOP) which are operated by the California Institute of Technology, under contract with the National Aeronautics and Space Administration. This paper includes data collected by the Kepler mission and obtained from the MAST data archive at the Space Telescope Science Institute (STScI). Funding for the Kepler mission is provided by the NASA Science Mission Directorate. STScI is operated by the Association of Universities for Research in Astronomy, Inc., under NASA contract NAS 5–26555.

DATA AVAILABILITY AND SOFTWARE ACCESS

The data used in this article, that was collected by the Kepler mission, is publicly available on the MAST data archive (https://archive.stsci.edu/). Self written code can be openly accessed through github (https://github.com/HsynKon/CurrentModel) and EXOFAST can be openly accessed from NASA Exoplanet Archive (http://exoplanetarchive.ipac.caltech.edu/).

REFERENCES

Brown T.M., Charbonneau D., Gilliland, R.L., Noyes R.W., Burrows A., 2001, ApJ, 552, 699
Cardoso et al., 2018, Astrophysics Source Code Library, record ascl:1812.013
Eastman J., Gaudi B. S., Algol E., 2013, PASP, 125, 83
Fressin F. et al., 2013, ApJ, 766, 81
Foreman-Mackey et al., 2021, Journal of Open Source Software, vol. 6, issue 62, id. 3285
Harris C.R. et al., 2020, Nature, 585, 357–362
Huber D. et al., 2016, ApJS, 224, 2
J. D. Hunter, 2007, Computing in Science & Engineering, vol. 9, no. 3, pp. 90-95
Kluyver T. et al., 2016, In F. Loizides, B. Schmidt, eds. Positioning and Power in Academic Publishing: Players, Agents and Agendas. pp. 87–90.
Mendez A., 2011, A Mass Classification for both Solar and Extrasolar Planets., Planetary Habitability Laboratory
NASA Exoplanet Exploration https://exoplanets.nasa.gov/alien-worlds/ways-to-find-a-planet/ (accessed July 8, 2021)
NASA Exoplanet Archive, http://exoplanetarchive.ipac.caltech.edu/ (accessed July 8, 2021)
NASA Exoplanet Archieve, https://exoplanets.nasa.gov/exoplanet-catalog/5609/kepler-487-b/ (accessed January 28, 2021)
Nesvorný D., 2009, ApJ, 701, 1116
Pecaut M. J., Mamajek E. E., 2013, ApJS,208, 9
Price-Whelan A. M., et al., 2018, AJ, 156, 123
Püsküllü Ç., 2016, Graduate thesis, Çanakkale Onsekiz Mart University/Science Institute
Robitaille T. P. et al., 2013, A&A, A33 https://doi.org/10.1051/0004-6361/201322068
Saral G., 2012, Graduate thesis, Ankara University/Science Institute
Timothy D. Morton, Stephen T. Bryson, Jeffrey L. Coughlin, Jason F. Rowe, Ganesh Ravichandran, Erik A. Petigura, Michael R. Haas, Natalie M. Batalha, 2016, ApJ, 822, 86
Van Rossum G., Drake F. L., 2009, Scotts Valley, CA:CreateSpace
Winn J.N., 2010, arXiv1001.2010
Yu L. et al., 2018, AJ, 156, 127